Site-Specific Enthalpic Regulation of DNA Transcription at Bacteriophage λ O_R[†]

Kenneth S. Koblan and Gary K. Ackers*

Department of Biochemistry and Molecular Biophysics, Washington University School of Medicine, 660 South Euclid Avenue, Box 8231, St. Louis, Missouri 63110

Received July 15, 1991; Revised Manuscript Received October 1, 1991

ABSTRACT: Binding of *c*I repressor to DNA fragments containing the three specific binding sites of the right operator (O_R) of bacteriophage λ was studied in vitro over the temperature range 5–37 °C by quantitative footprint titration. The individual-site isotherms, obtained for binding repressor dimers to each site of wild-type O_R and to appropriate mutant operator templates, were analyzed for the Gibbs energies of intrinsic binding and pairwise cooperative interactions. It is found that dimer affinity for each of the three sites varies inversely with temperature, i.e., the binding reactions are enthalpy driven, unlike many protein–DNA reactions. By contrast, the magnitude of the pairwise cooperativity terms describing interaction between adjacently site-bound repressor dimers is quite small. This result in combination with the recent finding that repressor monomer–dimer assembly is highly enthalpy driven (with $\Delta H° = -16$ kcal mol^{-1}) [Koblan, K. S., & Ackers, G. K. (1991) *Biochemistry 30*, 7817–7821] indicates that the associative contacts between site-bound repressors that mediate cooperativity are unlikely to be the same as those responsible for dimerization. The intrinsic binding enthalpies for all three sites are negative (exothermic) and nearly temperature-invariant, indicating no heat capacity changes on the scale of those inferred in other protein–DNA systems. However, the three operator sites are affected differentially by temperature: the intrinsic binding free energies for sites O_R1 and O_R3 change in parallel over the entire range, $\Delta H°_{O_R1} = -23.3 \pm 4.0$ kcal mol^{-1} and $\Delta H°_{O_R3} = -22.7 \pm 1.2$ kcal mol^{-1}. By contrast, the data for binding at O_R2 yields $\Delta H°_{O_R2} = -14.7 \pm 1.4$ kcal mol^{-1}. The ability of *c*I repressor to discriminate between the three operator sites is thus controlled by temperature since cooperativity terms are essentially temperature-invariant. The possible origins of these effects are discussed.

Regulation of prokaryotic and eukaryotic gene expression is often mediated by the control of transcription. Mechanisms for this regulation originate from a diverse array of protein factors (allosteric repressors, activators) and specific DNA sequences. Gene control systems may contain multiple DNA operators at which a family of structurally related proteins interacts. The regulatory proteins often bind DNA as dimers, either as homodimers (e.g., λ *c*I and *cro* repressors) or as heterodimers between two members of the same family (e.g., the mammalian JUN/FOS family) (Chiu et al., 1989; Schutte et al., 1989). Cooperative interactions between regulatory proteins bound to multiple DNA sites are often crucial in the functional cycle of this class of "macromolecular switches". Unique resolution of the intrinsic binding and cooperative interaction free energies as well as determination of the enthalpies and entropies for multisite systems is critical to understanding the physical mechanisms of gene control.

This laboratory has been carrying out a series of detailed studies on the energetics of interactions between *c*I repressor and the right operator region (O_R)[1] of bacteriophage λ (Ackers et al., 1982, 1983; Shea & Ackers, 1985; Brenowitz et al., 1986a,b, 1989; Senear et al., 1986; Senear & Ackers, 1990; Beckett et al., 1991; Koblan & Ackers, 1991a,b). The λ system is a prototype for understanding cooperativity in gene control systems. Interactions of *c*I and *cro* repressors, with the three operator sites of O_R, control the epigenetic switchover between lysogenic and lytic modes of the phage life cycle [see Ptashne (1986) for review]. Cooperative interactions between *c*I dimers bound to adjacent operator sites are crucial to maintenance of a stable lysogenic state and an efficient switchover to the lytic state during induction (Johnson et al., 1979; Ackers et al., 1982; Shea & Ackers, 1985). The footprint titration technique, a rigorous method capable of distinguishing interactions at individual sites, allows resolution of each macromolecular interaction. Quantitative measurement of the relevant protein dimerization energetics is also a necessity for correct resolution of the binding and cooperativity constants in this class of protein–DNA regulatory complexes (Beckett et al., 1991; Koblan & Ackers, 1991b).

The temperature dependence of *c*I dimerization has been presented elsewhere (Koblan & Ackers, 1991a). In the present study, we have employed quantitative footprint titration to obtain a full thermodynamic profile ($\Delta G°$, $\Delta H°$, and $\Delta S°$) for the *c*I repressor–O_R interactions. At each temperature, the individual-site isotherms for wild-type O_R and three additional (mutant) operators were analyzed to resolve the Gibbs free energies of *c*I binding to each site and the cooperative free energies for pairwise interactions between adjacent sites. Determination of the corresponding equilibrium constants as a function of temperature has permitted resolution of their enthalpic and entropic components. These results indicate that cooperativity is maintained over the entire range investigated and that it is insensitive to variations in temperature. Binding

[†] Supported by National Institutes of Health Grants GM39343 and R37-GM24486.

* Correspondence should be addressed to this author.

[1] Abbreviations: DNase I, bovine pancreas deoxyribonuclease I (EC 3.1.21.1); bis(acrylamide), *N,N'*-methylenebis(acrylamide); TEMED, *N,N,N',N'*-tetramethylethylenediamine; BSA, bovine serum albumin; CT-DNA, calf thymus DNA; bp, base pair(s); O_R, λ right operator; Tris, tris(hydroxymethyl)aminomethane; Bistris, [bis(2-hydroxyethyl)-amino]tris(hydroxymethyl)methane.

0006-2960/92/0431-57$03.00/0

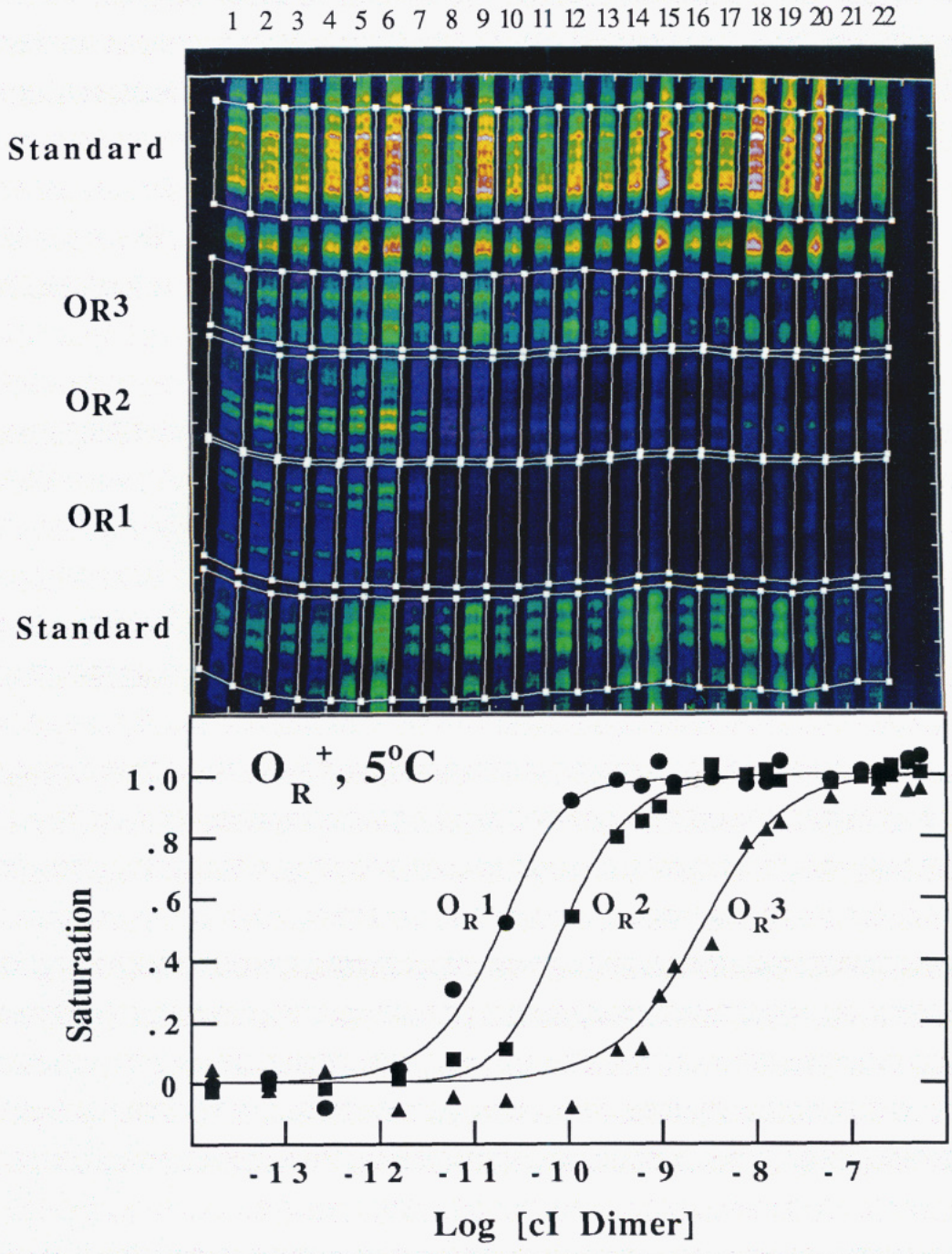

FIGURE 1: (Top) False color image of footprint titration of an O_R^+ operator. Reaction conditions are 5 °C and standard assay buffer, pH 7. Blocks of bands corresponding to the operator sites and to standards are indicated (see text). The white squares indicate coordinate points chosen by the investigator. White contour lines indicate the areas for which the integrated OD was determined. Lane 1 contains no added *c*I. Repressor concentration increases from left to right. (Bottom) Individual-site binding data obtained from the autoradiogram shown above. Symbols: (●) site O_R1; (■) site O_R2; (▲) site O_R3. Solid curves represent simultaneous analysis of the data for O_R^+, O_R1^-, $O_R1^-3^-$, and O_R2^- operators at this condition. Interaction parameters are in Table II.

to each of the three sites is enthalpically driven, and the reaction enthalpies are temperature-independent. Since dimer formation is also enthalpically driven (Koblan & Ackers, 1991a), *c*I dimerization and its binding to DNA are linked significantly through their temperature dependencies.

Materials and Methods

Chemical Reagents. α-^{32}P-labeled deoxyribonucleotides (3000 Ci/mmol) were from Amersham; unlabeled deoxyribonucleotides were from P-L Biochemicals. Electrophoresis-grade acrylamide, bis(acrylamide), ammonium persulfate, and TEMED were from Bio-Rad. Urea was sequenal grade from Pierce Chemical Co. Acrylamide, bis(acrylamide), and urea were deionized with Bio-Rad AG501-X8 resin prior to use. CsCl was biochemical grade from Gallard-Schlesinger. All other reagents were reagent or analytical grade.

Biological Materials. Restriction endonucleases were from IBI or New England Biolabs. The large (Klenow) fragment of *Escherichia coli* DNA polymerase I and bovine serum albumin (BSA) (acetylated nucleic acid enzyme grade) were from Bethesda Research Labs (BRL). Calf thymus DNA (CT-DNA) was from P-L Biochemicals. Bovine pancreas deoxyribonuclease I (DNase I, code D) from Worthington was stored as a 2 mg/mL stock solution in 150 mM NaCl and 50% glycerol at −70 °C and diluted appropriately into assay buffer

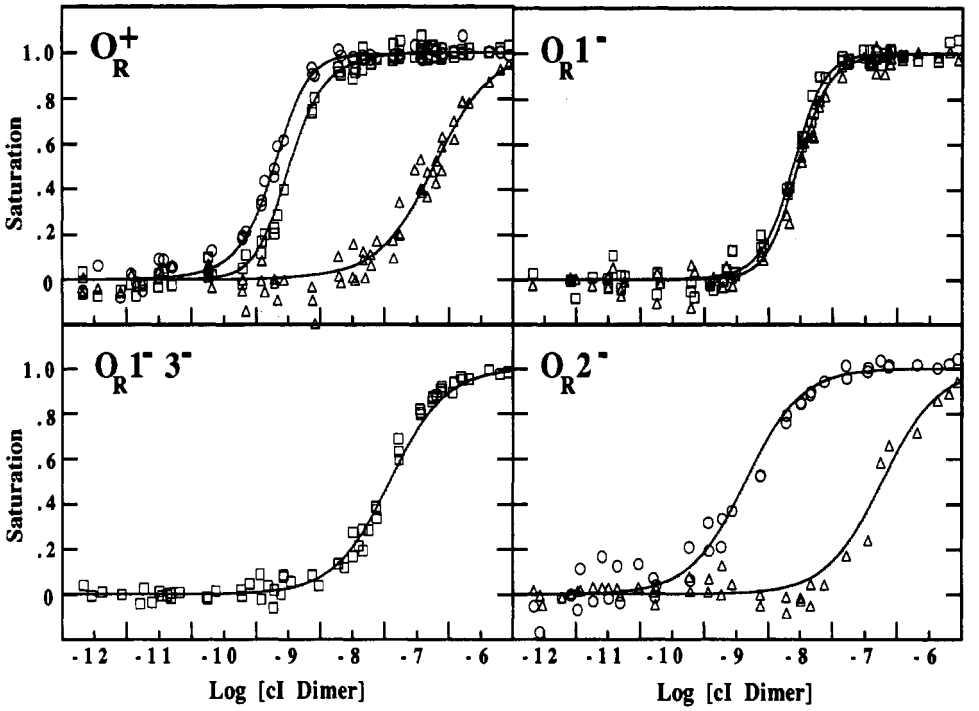

FIGURE 2: Individual-site binding data at 37 °C for interaction of λ cI repressor with O_R^+, and reduced valency O_R mutants, at pH 7.00 and 200 mM KCl. These data represent 11 separate experiments. Panels show O_R^+, O_R1^-, $O_R1^-3^-$, and O_R2^- operators, respectively. Symbols: (○) site O_R1; (□) site O_R2; (△) site O_R3. Solid curves represent simultaneous analysis of the data in all panels.

less BSA and CT-DNA, immediately prior to exposure. The relative catalytic activity of DNase I was determined at each temperature in order to obtain constant backbone nicking over the entire range.

cI protein used in these studies was purified as previously described (Johnson et al., 1980). Purity was greater than 95% as judged by electrophoresis on SDS gels but only 56% active, based on stoichiometry experiments of the type described by Sauer (1979) and Johnson (1980) and based on $\epsilon^{280nm}_{mg/mL\cdot cm}$ = 1.18. Total active monomer concentrations were calculated from the stoichiometry experiments. The monomer–dimer equilibrium constant was determined at each condition studied (Koblan & Ackers, 1991a).

Preparation of Operator DNA. Plasmids were purified by the procedure of Birnboim and Doly (1979) followed by CsCl density centrifugation (Maniatis et al., 1982). Plasmid pKB252 (Backman et al., 1976) containing the wild-type (O_R^+) λ operator was a gift from H. Nelson and R. Sauer. Three reduced-valency mutant templates were used. Each contains a single base-pair substitution in one or two of the operator binding sites, which eliminate (⁻) site-specific repressor ligation. Plasmids which contained mutant operator regions, pBJ301 (O_R1^-), pBJ303 ($O_R1^-3^-$), and pBJ306 (O_R2^-) (Meyer et al., 1980), were gifts from J. Eliason and M. Ptashne. Operator-containing fragments were excised from the plasmids with *Bgl*II (bp 38 103 in the λ *cro* gene) and *Pst*I (bp 37 001 in the λ cI gene), yielding 1102 bp fragments. Preparation and radiolabeling of the restriction fragments were by standard procedures (Maniatis et al., 1982). Specific radioactivity of freshly labeled DNA [typically (7–10) × 10^6 Ci/mol] was used to estimate the operator concentration in binding experiments.

Individual-Site Binding Experiments. Quantitative DNase I footprint titration experiments were conducted (Brenowitz et al., 1986a), with slight modifications. Binding experiments were carried out in assay buffer consisting of 10 mM Bistris, 200 mM KCl, 2.5 mM $MgCl_2$, 1.0 mM $CaCl_2$, 100 μg/mL BSA, and 2 μg/mL CT-DNA (sonicated) and pH 7.00 ± 0.01 at the temperature of the binding experiments. Reaction mixtures containing 15 000–25 000 cpm of ^{32}P-labeled operator DNA (less than 10 pM in operator-containing fragments) in a volume of 200 μL were incubated for 1–2 h prior to DNase exposure. In order to sample cI occupancy of binding sites, 5 μL of DNase solution (preequilibrated at the temperature of interest) was added to each sample. The relative catalytic activity of DNase I increased with increasing temperature. To maintain constant exposure, the DNase I concentration was varied (50–125 ng/mL final) to correct for the increased backbone nicking as the temperature increased. The pattern of DNase nicking was constant at every experimental condition, indicating no significant temperature-dependent effects on DNA conformation or cI repressor–DNase I interaction. All DNase exposures were conducted for 1.0 min prior to quenching. Electrophoresis on 8% acrylamide–urea gels and autoradiography were as described previously (Brenowitz et al., 1986a).

Optical density of the film was measured in two dimensions by an Eikonix 1412 CCD digital camera.[2] Scanning approximately a 23 × 23 cm area of an autoradiogram at a resolution of 150 μm produces a 1500 × 1500 data point array at a resolution of 12 bits per pixel. Linearity of camera response was determined (before and after data collection) by scanning a precalibrated step wedge (Kodak). The optical density array corresponding to 150-μm pixels on the autoradiogram is processed interactively with programs developed in this laboratory. Fractional operator-site occupancy is monitored by the ratio of integrated optical density of a series of bands within a binding site to that of similar bands outside the binding site (Brenowitz et al., 1986a).

Figure 1 shows a representative titration of wild-type, O_R^+ operator. Repressor binding to O_R1, O_R2, and O_R3 is reflected

[2] A one-dimensional scan of the autoradiogram has been found inadequate to quantitate the number and density of DNA fragments in all regions of a gel lane. Neither the maximum peak height nor a single-dimension peak profile can provide an accurate representation of the density of a band (Brenowitz et al., 1986a).

by increasing protection in those sites. Standard regions outside the binding sites are used to normalize the degree of protection to total DNA loaded in each lane (Brenowitz et al., 1986a). Absence of protection outside the operator sites, at every experimental condition, indicates that the repressor maintains high specificity over the entire temperature range, 5–37 °C. Under conditions in these studies, no nonspecific binding to DNA regions outside the specific sites could be detected (i.e., the ratio of specific to nonspecific affinities is at least 10^7). At 20 °C that translates into a difference in free energy between binding to O_R1 and binding to nonspecific DNA of approximately 9 kcal mol^{-1}, which is consistent with values recently determined for *c*I binding nonspecifically to fragments of pBR322 DNA (Senear & Batey, 1991). High carrier DNA concentrations (CT-DNA) maintained the unliganded DNA concentration constant, even as the operator sites were filled. Controls verified that the unlabeled CT-DNA does not affect the binding of *c*I repressor to the single-site O_R1 (range 5–20 °C).

The signal in a footprint titration experiment is the degree of protection at a given site from DNase I cleavage provided by a given concentration of ligand. Protection at a given site is linearly related to fractional saturation. Since the saturating concentration of ligand does not result in complete protection, the apparent fractional saturation at each site does not span the range from 0 to 1. For this reason, the data are analyzed as a transition curve, and the end points for each individual-site isotherm are included as adjustable parameters to be resolved by the least-squares analysis. This treatment dictates that each experiment be conducted over a wide concentration range (e.g., 10^{-12}–10^{-6} M) in order to obtain reliable transition end points and energetics from the complex curve shapes.

Numerical Analysis. Data were analyzed according to the appropriate binding functions using nonlinear least-squares parameter estimation (Johnson et al., 1976; Johnson & Frasier, 1985) to determine the best-fit model parameters which yield a minimum in the variance. A resolved variance ratio is predicted by an *F* statistic to determine the worst case joint confidence intervals for the fitted parameters. Confidence intervals (67%) correspond to approximately one standard deviation.

Because of the high statistical correlation between the constants to be resolved, it is necessary to combine results from experiments on an appropriate set of templates in order to obtain unique and physically correct values of the Gibbs free energy terms (Shea, 1983; Brenowitz et al., 1986a; Senear et al., 1986). Independent data sets are analyzed as a composite to resolve the model parameters that simultaneously minimize the least-squares value for the entire composite. In order to determine the five microscopic interaction constants, binding experiments were conducted on O_R^+ and a set of reduced valency mutants: O_R1^-, O_R2^-, and $O_R1^-3^-$ (Figure 2). It is assumed that interactions at any competent binding site are quantitatively unperturbed by the mutation [assumption 7 of Ackers et al. (1982); Senear et al., 1986]. Validity of this assumption in any given study requires the identification of a self-consistent "basis set" of reduced-valency operators (see Discussion).

At every experimental condition in this study, results of duplicate experiments on all four templates (eight separate scans) were incorporated in the simultaneous analysis to resolve the five parameters of Table I. Weighting factors were employed in the analysis of each composite data set from different experiments (wild-type and mutant templates) to account for variations in experimental noise. Appropriate weighting factors were obtained by first analyzing each experiment independently to obtain the best "phenomenological" fit (Senear et al., 1986; Koblan et al., 1991). Cooperativity terms ΔG_{ij} were input as fixed parameters in these separate analyses. Free energies ΔG_1, ΔG_2, and ΔG_3 and the titration end points were fitted parameters (Brenowitz et al., 1986a). Variances found for the best combination of ΔG_{ij} terms were taken to define precision of that set of individual data points. Weighting factors (Bevington, 1969) were calculated by

$$\sigma_{ij} = N_t(1/\sigma_j^2)/\sum_j(N_j/\sigma_j^2) \quad (1)$$

where σ_{ij} is the weight assigned to data point *i* of experiment *j*, σ_j^2 and N_j are the variance and number of data points for experiment *j*, respectively, and $N_t = \sum_j N_j$. Computations were performed on a Hewlett-Packard 9000 computer.

Table I: Microscopic Configurations and Associated Free Energy Contributions for the λ *c*I Repressor–Operator System, O_R[a]

species	operator configurations O_R1		O_R2		O_R3	free energy contributions
1	0		0		0	reference
2	R_2		0		0	ΔG_1
3	0		R_2		0	ΔG_2
4	0		0		R_2	ΔG_3
5	R_2	↔	R_2		0	$\Delta G_1 + \Delta G_2 + \Delta G_{12}$
6	R_2		0		R_2	$\Delta G_1 + \Delta G_3$
7	0		R_2	↔	R_2	$\Delta G_2 + \Delta G_3 + \Delta G_{23}$
8	R_2	↔	R_2		R_2	$\Delta G_1 + \Delta G_2 + \Delta G_3 + \Delta G_{12}$
9	R_2		R_2	↔	R_2	$\Delta G_1 + \Delta G_2 + \Delta G_3 + \Delta G_{23}$

[a] Individual operator sites are denoted by 0 if vacant or R_2 if occupied by *c*I dimers. ΔG_{ij}'s are free energies of cooperative interaction between liganded sites (↔). Each intrinsic free energy, ΔG_1, ΔG_2, or ΔG_3, reflects the intrinsic binding to the respective site. ΔG_{ij} is the difference between the total free energy to fill two adjacent sites *i* and *j* simultaneously and the sum of the intrinsic binding energies ($\Delta G_i + \Delta G_j$). Free energies are related to the corresponding microscopic equilibrium constants, k_i, by $\Delta G_i = -RT \ln k_i$. Species 8 and 9 are isomeric forms of the same triliganded operator complex but have different configurations of pairwise cooperativity.

At all temperatures the approximation that $[P]_{total} \approx [P]_{free}$ is accurate because operator concentrations were low relative to the equilibrium constants. Free dimer concentrations were calculated directly from the truncated repressor conservation equation $R_t = R_1 + 2R_2$ (monomer units) and knowledge of the dimer dissociation constant $k_d = [R_1]^2/[R_2]$, as experimentally determined (Koblan & Ackers, 1991a). Physical–chemical dissection of coupled protein–protein and protein–DNA interactions must include quantitative measurement of the functionally relevant polymerization reactions.

Interaction Free Energies. Gibbs energies for both site-specific repressor binding and pairwise interactions were determined by analyzing data according to the appropriate expressions for each of the individual sites. These expressions are formulated from the relative probabilities, f_s, of the various operator configurations:

$$f_s = \frac{\exp(-\Delta G_s/RT)[R_2]^j}{\sum_s \exp(-\Delta G_s/RT)[R_2]^j} \quad (2)$$

ΔG_s is the sum of free energy contributions for configuration *s* (Table I), *R* is the gas constant, *T* is the absolute temperature, $[R_2]$ is the concentration of free dimer, and *j* is the repressor stoichiometry in operator configuration *s*. Interaction of *c*I dimers with the three operator sites yields nine possible configurations (Table I) (Shea, 1983). Species 8 and 9 of Table I are isomeric forms of the same triliganded operator complex but have different configurations of pairwise cooperativity. This specification of the operator configurations has been termed the "extended pairwise cooperativity model"

Table II: Temperature Dependence of Microscopic Gibbs Energies of Repressor–O_R Interactions[a]

T (°C)	ΔG_1	ΔG_2	ΔG_3	ΔG_{12}	ΔG_{23}	s^b
37	−12.5 ± 0.3	−10.5 ± 0.2	−9.5 ± 0.2	−2.7 ± 0.3	−2.9 ± 0.5	0.047
30	−12.4 ± 0.3	−10.6 ± 0.2	−9.9 ± 0.2	−2.6 ± 0.3	−2.7 ± 0.5	0.058
20	−13.2 ± 0.3	−10.7 ± 0.3	−10.2 ± 0.3	−3.0 ± 0.6	−3.0 ± 0.7	0.078
10	−13.3 ± 0.2	−10.8 ± 0.2	−10.7 ± 0.2	−2.6 ± 0.4	−2.9 ± 0.4	0.049
5	−13.5 ± 0.3	−11.0 ± 0.2	−10.9 ± 0.2	−1.9 ± 0.3	−2.5 ± 0.4	0.048

[a] Standard Gibbs energies (in kilocalories per mole ± 67% confidence intervals) of repressor–O_R interactions, obtained by simultaneous analysis of O_R^+ and reduced valency mutant binding data. Reaction conditions were pH 7.00, 200 mM KCl, and T (°C) as indicated. [b] Square root of the variance from the simultaneous analysis.

(Senear & Ackers, 1990). Five microscopic free energy terms can contribute to each species, ΔG_s. The three intrinsic free energies, ΔG_1, ΔG_2, and ΔG_3, reflect binding to each respective site in the absence of binding at any others. Cooperativity terms ΔG_{12} and ΔG_{23} denote the excess free energy for binding to two sites simultaneously. By definition ΔG_{ij} is the difference between the total free energy to fill two adjacent sites i and j simultaneously (ΔG_T) and the sum of the intrinsic binding energies ($\Delta G_i + \Delta G_j$). The DNase I footprint titration technique resolves the fractional occupancies of each operator site, $\bar{Y}_i$, as a function of free [R_2]. Mathematical expressions for the individual-site isotherms are constructed by summation of the probabilities f_s, for the respective configurations of Table I (e.g., for a wild-type operator):

$$\bar{Y}_{O_R1} = f_2 + f_5 + f_6 + f_8 + f_9 \quad (3a)$$

$$\bar{Y}_{O_R2} = f_3 + f_5 + f_7 + f_8 + f_9 \quad (3b)$$

$$\bar{Y}_{O_R3} = f_4 + f_6 + f_7 + f_8 + f_9 \quad (3c)$$

Relationships are obtained in an analogous manner for mutant operators where specific binding sites have been eliminated by single base-pair substitutions. For example, only configurations 1, 2, 4, and 6 (Table I) can exist for an O_R2^- mutant operator.

Data were analyzed simultaneously, using the appropriate binding expressions in the form of eq 3a–c. Symbols represent individual data points while each curve represents an isotherm for one of the operator sites calculated using the resolved parameters from the simultaneous analysis.

Results

Results are given in Table II for all conditions. The steepness of the isotherms for O_R1 and O_R2 provides a visual demonstration of the cooperative ligation at both sites (Figures 2 and 3). Analysis of individual O_R^+ experiments (each condition) always yielded a minimum variance for $\Delta G_{ij} < 0$. This trend leads to greater confidence in the cooperative nature of the binding than indicated by the confidence limits for individual experiments; these could not, in all cases, exclude $\Delta G_{ij} = 0$. Previous studies have demonstrated an asymptotic limit to the shapes of isotherms for energetically coupled sites in this system (Senear et al., 1986). The data for the present study lie within the range of these asymptotic limits (calculations not shown).

Temperature-Linked Effects. Repressor binding as a function of temperature is shown in Figure 3. Each panel displays the self-consistent results from duplicate sets of four separate experiments (O_R^+ and three reduced-valency mutant templates) at each temperature. The symbols represent individual data points from binding experiments conducted on O_R^+ templates, while the solid curves represent the combined analysis of all DNA templates. The increase in affinity at each of the three sites as temperature decreases is clearly indicated by the leftward shifts in positions of the curves.

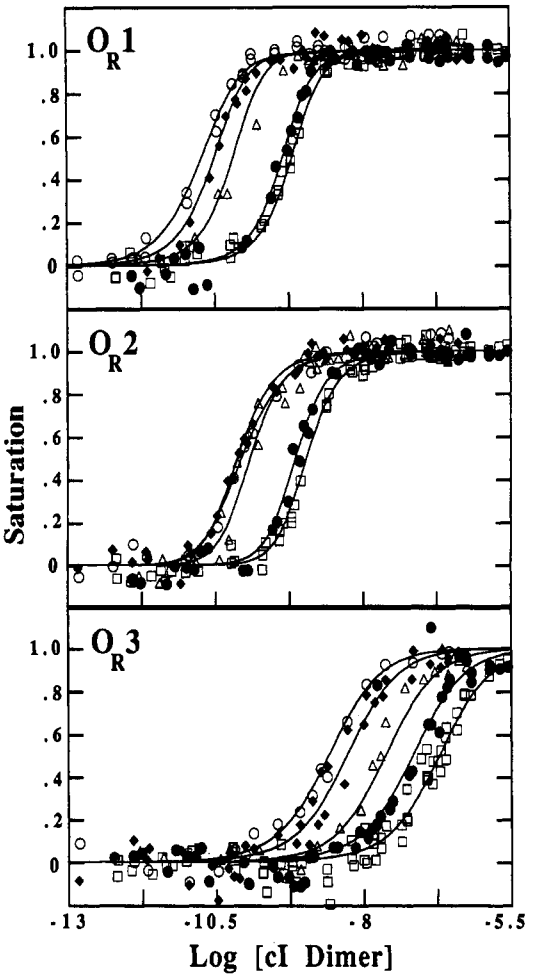

FIGURE 3: Individual-site isotherms for cooperative binding of λ cI repressor to O_R as a function of temperature. Reaction conditions are pH 7.00, standard assay buffer (see text), and temperature as indicated. Panels (from top to bottom) are for O_R1, O_R2, and O_R3, respectively, at (□) 37 °C, (●) 30 °C, (△) 20 °C, (◆) 10 °C, and (○) 5 °C. Solid curves represent the simultaneous analysis of experimental data for wild-type and reduced valency operators as described in the text. The estimated Gibbs interaction energies are in Table II.

The individual-site binding isotherms (for wild-type and mutant operators) from each experiment provide a measure of the total chemical work available to the system. This chemical work (Gibbs energy) for binding 1 mol of cI repressor at each respective site while stoichiometric amounts of ligand are also bound to other sites is the *individual-site "loading" free energy* $\Delta G_{L,i}$ (Ackers et al., 1983). The loading free energy includes all energetic contributions that affect binding of a ligand at site i. The loading free energies can be evaluated directly from the individual-site isotherms in a model-independent manner by numerical integration:

$$\Delta G_{L,i} = RT \ln \bar{X}_i = RT \int_0^1 \ln X \, d\bar{Y}_i \quad (4)$$

Table III: Individual-Site Loading Free Energies ($\Delta G_{L,i}$) from Separate Experiments for Each Operator[a]

operator	expt[b]	$\Delta G_{L,1}$	$\Delta G_{L,2}$	$\Delta G_{L,3}$
O_R^+	i	−13.05	−12.60	−9.61
	ii	−13.28	−12.67	−9.80
	model[c]	−13.08	−12.66	−9.69
O_R1^-	i		−11.58	−11.39
	ii		−11.53	−11.18
	model[c]		−11.53	−11.38
O_R2^-	i	−12.46		−9.47
	model[c]	−12.54		−9.66
$O_R1^-3^-$	i		−10.62	
	ii		−10.52	
	model[c]		−10.54	

[a] $\Delta G_{L,i}$'s (in kilocalories per mole) were calculated by numerical integration using eq 4. Reaction conditions were pH 7.00, 200 mM KCl, and 37 °C. [b] Separate experiments are denoted i or ii. The fractional saturation data for each isotherm were used in the calculation. [c] Calculated from isotherms resolved from simultaneous analysis of data from all operators.

Table IV: Temperature Dependence of Loading Free Energies, $\Delta G_{L,i}$[a]

T (°C)	$\Delta G_{L,1}$	$\Delta G_{L,2}$	$\Delta G_{L,3}$
37	−13.1 ± 0.2	−12.7 ± 0.2	−9.7 ± 0.3
30	−13.0 ± 0.2	−12.6 ± 0.2	−9.9 ± 0.2
20	−13.7 ± 0.2	−13.2 ± 0.2	−10.2 ± 0.2
10	−13.6 ± 0.2	−13.0 ± 0.2	−10.7 ± 0.2
5	−13.6 ± 0.2	−12.7 ± 0.2	−10.9 ± 0.2

[a] Values in kilocalories per mole. Calculated from isotherms resolved from simultaneous analysis of data from all operators (O_R^+, O_R1^-, O_R2^-, $O_R1^-3^-$).

where $\bar{X}_i$ is the median ligand activity and $\bar{Y}_i$ is the fractional saturation at ligand activity X [Wyman, 1964; see Ackers et al. (1983) for analysis in terms of individual sites]. Independent of any uncertainties which may exist in estimated values of model parameters, the individual-site loading free energies are precisely determined from the observed data points using eq 4. As illustrated in Table III, there is close agreement between separate experiments and with the isotherms resolved from the model-dependent nonlinear least-squares analysis. Titration end points resolved by the best "phenomenological" fits were used in the calculations. Table IV presents the loading free energies ($\Delta G_{L,i}$) for all three sites as a function of temperature.

van't Hoff plots for each individual site are shown in Figure 4. The intrinsic binding energies are well resolved, as indicated by the narrow confidence intervals (i.e., the error bars). Table V compares the Gibbs energies for intrinsic-site binding as a function of temperature for two mutant operators and the model-dependent values resolved from simultaneous analysis of data from all templates at a given condition. Examination of the $O_R1^-3^-$ mutant operator reflects only the intrinsic binding free energy ΔG_2. Similarly, the O_R2^- mutant will reflect the intrinsic binding free energies ΔG_1 and ΔG_3. Values resolved for mutant operators fall within the error bars of Figure 4.

Binding to each of the three sites in enthalpy driven over the entire range. These results are strikingly different from the results obtained by Record and co-workers for the binding of *lac* repressor and *Eco*RI endonuclease to their specific recognition sites as a function of temperature (range 0–41 and 4.7–37 °C, respectively) (Ha et al., 1989). Binding reactions of these proteins are characterized by a large negative apparent heat capacity change; i.e., the standard enthalpy of association is temperature-dependent. Those binding reactions appear to be entropy driven at low temperatures and enthalpy driven at higher temperatures under the assumption that no dissociation or further oligomerization occurs. The results of the present study are similar to those obtained by Dabrowiak and co-workers for the temperature dependence of DNA binding by the drug netropsin and the dipeptide lexitropsin (Dabrowiak et al., 1990).

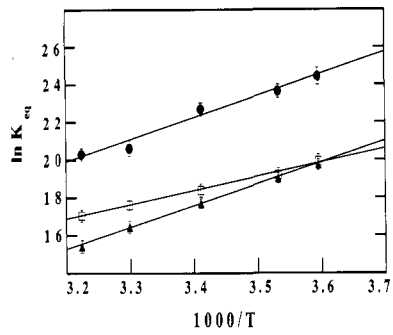

FIGURE 4: van't Hoff analysis for the site-specific interactions of λ *c*I repressor at O_R: (●) O_R1; (□) O_R2; (▲) O_R3. The solid lines were determined by linear regression to the data points for each site. Error bars indicate 67% confidence intervals.

Table V: Intrinsic-Site Free Energies from Mutant Operators and Composite Analysis[a]

T (°C)	expt	$O_R1^-3^-$ operator ΔG_2,	O_R2^- operator ΔG_1	ΔG_3
37	single operator	−10.6 ± 0.3	−12.5 ± 0.3	−9.6 ± 0.3
	composite	−10.5 ± 0.2	−12.5 ± 0.3	−9.5 ± 0.2
30	single operator	−10.7 ± 0.2	−12.4 ± 0.3	−9.9 ± 0.2
	composite	−10.6 ± 0.2	−12.4 ± 0.3	−9.9 ± 0.2
20	single operator	−10.8 ± 0.3	−13.3 ± 0.3	−10.2 ± 0.3
	composite	−10.7 ± 0.3	−13.2 ± 0.3	−10.2 ± 0.3
10	single operator	−10.8 ± 0.2	−13.3 ± 0.3	−10.7 ± 0.2
	composite	−10.8 ± 0.2	−13.3 ± 0.2	−10.7 ± 0.2
5	single operator	−11.0 ± 0.2	−13.5 ± 0.3	−11.0 ± 0.2
	composite	−11.0 ± 0.2	−13.5 ± 0.3	−10.9 ± 0.2

[a] Values in kilocalories per mole. Composite refers to simultaneous analysis of data from all operators (O_R^+, O_R1^-, O_R2^-, $O_R1^-3^-$) which resolves the five parameters defined in Table I.

Our results are in qualitative agreement with an early report that the stability of the *c*I repressor–operator complex decreases as a function of increasing temperature (Ptashne, 1967). The repressor maintains its relative order of affinities, $O_R1 > O_R2 > O_R3$, over the range studied. Evaluation of differences between the cooperative free energies is less certain due to the larger errors in the ΔG_{12} and ΔG_{23} terms. The confidence intervals for these parameters reflect all systematic differences between separate experiments, and between the different operators, as well as the imprecision of individual experiments. While it is clear that the magnitudes of the cooperativity terms ΔG_{12} and ΔG_{23} are quite small, no interpretable pattern is readily apparent for their temperature dependence.

Discussion

In this study we have employed quantitative footprint titration to measure the effects of temperature on interactions of the λ *c*I repressor and O_R using methods developed previously in this laboratory. Simultaneous analysis of wild-type and reduced-valency mutant operators (Senear et al., 1986) has allowed us to study the effects of various thermodynamic parameters on the energetics of site-specific recognition and cooperative interactions in this system. Independent measurement of the thermodynamics of repressor dimerization under identical solution conditions (Koblan & Ackers, 1991a) permits us to separate uniquely the roles that temperature plays

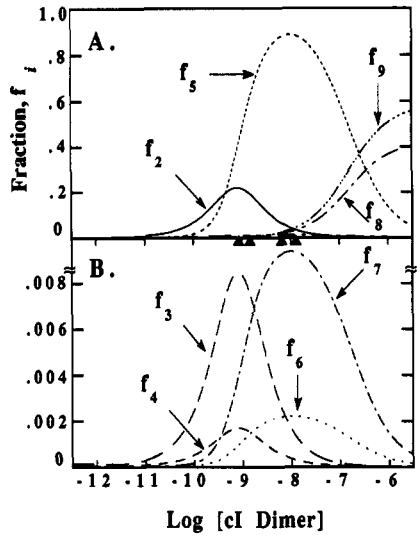

FIGURE 5: Species populations for the different configurations of bound sites (Table I) at 37 °C and 200 mM KCl, pH 7.00. Singly liganded species are f_2, f_3, and f_4; doubly liganded species are f_5, f_6, and f_7; triply liganded species are f_8 and f_9. (A) Distributions for all nine species (species 1, reference state) are from resolved equilibrium constants and the statistical thermodynamic model of Table I. Symbols (▲) indicate maxima for individual ligation species which are not significantly populated. (B) Distribution of species which are not highly populated in (A). Note ordinate scale is 1/100 of (A).

in these coupled protein–protein and protein–DNA association reactions.

Validity of Analysis Procedures. The ability of the individual-site binding curves for each site to resolve the microscopic interaction constants relies on the use of reduced-valency mutant operators in the simultaneous analysis. Critical implicit assumptions in this analysis are (a) that all interactions at the remaining sites are quantitatively unperturbed by single base-pair substitution in the mutated site(s) and (b) that the mutations actually eliminate binding at those sites. There exist a number of mutant operators (O_R2^-, $O_R1^-3^-$) which satisfy criterion b under all conditions examined to date. The $O_R1^-2^-$ mutant operator previously employed in this laboratory (Senear & Ackers, 1990) was not included in the present study nor in our previous study on KCl effects (Koblan & Ackers, 1991b). In our KCl study both the $O_R1^-2^-$ and O_R1^- templates were considered unreliable because base substitution at the mutation point contained in site O_R1 had previously been found to reduce, but not eliminate, the specific O_R1 binding [see Figure 5 of Senear and Ackers (1990)]. In initial experiments, the value we obtained for cI binding to site 1 of the O_R1^- template at 50 mM KCl was −11 kcal mol^{-1}. We therefore concluded that this template was not acceptable for studies at low salt conditions. A recent study on KCl effects from a different laboratory (Senear & Batey, 1991) did incorporate the O_R1^- template. Comparison of results from the two studies suggests that a main consequence of incorporating the O_R1^- template may have been to produce an anomalously low value of the intrinsic-site free energy ΔG_3 at the lowest salt concentrations (e.g., −12.1 kcal mol^{-1} vs −13.3 kcal mol^{-1} at 50 mM KCl). Using experimental values of repressor dimerization constants (Koblan & Ackers, 1991a), a simulation of the values found by Senear and Batey (their Table II) indicates that a binding free energy of −10 kcal mol^{-1} to site 1 of the O_R1^- template would propagate as 1.1 kcal mol^{-1} into the apparent ΔG_3, accounting for the difference between −12.1 kcal mol^{-1} and −13.3 kcal mol^{-1}. The findings from our KCl study, that sites O_R1 and O_R3 exhibit parallel salt dependencies (Koblan & Ackers, 1991b), would not obtain had the O_R1^- template been included in that analysis. At every condition in the present study, simultaneous analysis of any combination of wild-type and mutant operators (e.g., the set O_R^+, $O_R1^-3^-$, O_R2^- or the set O_R^+, O_R1^-, O_R2^-) always resolved the same values, given in Table II. This internal consistency addresses not only the accuracy and precision obtainable with the footprint titration technique but also the validity of the model employed.

Resolution of Species Distributions. Individual-site isotherms (Figures 2 and 3) as experimentally determined are uniquely defined by concentrations of the various liganded species as a function of ligand activity (eq 3a–c). The probability f_s (eq 2) of each of the nine microscopic configurations of Table I represents the fraction of operators present in that configuration at a given concentration of repressor dimer. The distribution of ligation species according to the extended pairwise model (Table I) is shown in Figure 5.

When all potential single ligation events (species 2, 3, and 4 of Table I) are considered, it is clear that species 2 (cI bound to O_R1) dominates this ligation state. For all doubly liganded species only species 5 (cI bound and cooperatively interacting at sites O_R1 and O_R2) is significantly populated. It is important to note that the doubly liganded species 7 (cI bound and cooperatively interacting at sites O_R2 and O_R3) is never highly populated (Figure 5B). In this system species 7 and in particular the ΔG_{23} term make virtually no contribution to the individual-site isotherms. However, experiments conducted on the reduced-valency template O_R1^- do allow resolution of the ΔG_{23} term.

The nature of energetic coupling in this and similar systems [e.g., Ackers and Smith (1987)] dictates that the intermediate ligation states (j = 1 or 2) are highly unpopulated or dominated by a single ligation species. The consequence is that it is extremely difficult to discern between mechanistic models which embody subtle differences between these unpopulated ligation species. Such is the case in the λ O_R system. Only by considering the three-site problem as a subset of two-site problems and employing reduced-valency templates (mutant DNA operators) are we able to resolve all of the relevant interaction parameters. In this regard, the individual-site loading free energies (Table III) provide an important model-independent constraint on the analysis.

The sum of individual-site loading free energies equals the total free energy of interaction within the system $\Delta G_T = \Delta G_{L,1} + \Delta G_{L,2} + \Delta G_{L,3}$. This total must reflect the product of the microscopic interaction constants resolved by any model-dependent analysis (e.g., for the extended pairwise model $\Delta G_T = -RT \ln [k_1k_2k_3(k_{12} + k_{23})]$). The sum of the $\Delta G_{L,i}$'s agrees closely with the sum of the model-dependent ΔG_i's and ΔG_{ij}'s (e.g., at 37 °C $\sum \Delta G_{L,i}$ = −35.4 kcal mol^{-1} vs $\sum \Delta G_{T\ \text{model-dependent}}$ = −35.3 kcal mol^{-1}). This close agreement provides an important verification that the model employed is physically relevant.

Temperature Effects on Repressor Binding. The Gibbs energies detailed in Table II demonstrate two fundamental results. First, the intrinsic association constants for repressor binding to the three sites of the right operator are sensitive to temperature. This temperature dependence is different among the three sites, indicating fundamental differences between them. Second, the Gibbs energies of cooperative interaction between O_R1 and O_R2, and between O_R2 and O_R3, are small and indistinguishable. Resolution of the cooperativity terms is not precise enough to determine whether there is any dependence on temperature. It is important to realize that discrimination between sites O_R1 and O_R3 is not intrinsically temperature-dependent but is effectively so because the in-

Table VI: Thermodynamic Linkages of O_R at pH 7, 20 °C, and 200 mM KCl[a]

system	$\Delta H°$ (kcal mol^{-1})	$T\Delta S°$ (kcal mol^{-1})	$\Delta\bar{\nu}_{H^+}$ absorbed	$\Delta\bar{\nu}_{KCl}$ released
O_R1	−23.3	−10.1	0.4	3.7
O_R2	−14.7	−4.0	1.1	5.2
O_R3	−22.7	−12.5	0.6	3.8
cooperativity	~0.0	+3.0	0.0	0.0
dimerization	−15.9	+4.9	0.3	−1.5

[a] $\Delta\bar{\nu}_{H^+} = (\mathrm{d} \ln k)/(\mathrm{d} \ln a_{H^+})$; $\Delta\bar{\nu}_{KCl} = (\mathrm{d} \ln k)/(\mathrm{d} \ln [KCl])$. Cooperativity denotes values derived from the cooperative interaction parameters ΔG_{12} and ΔG_{23}. Dimerization indicates the *c*I dimerization equilibrium.

teraction at O_R2 has a different linkage to temperature and repressor bound to site O_R2 interacts cooperatively with both O_R1 and O_R2 (Table IV).

Slopes of the curves in Figure 4 indicate a significant difference in the effect of temperature on binding at O_R1 and O_R3 compared to O_R2. The striking parallel between the temperature responses at sites O_R1 and O_R3 versus O_R2 follows the same pattern as previous results on *c*I binding to O_R: (a) as a function of pH (Senear & Ackers, 1990) and (b) as a function of [KCl] (Koblan & Ackers, 1991b). These findings of the three studies from this laboratory are summarized in Table VI. The effect of protons on O_R1 and O_R3 binding (pH 6–7 range) was found to change in parallel but to differ from the effects on binding to O_R2. The [KCl] dependencies of O_R1 and O_R3 binding (50–200 mM range) both exhibited an apparent release of 3.7 ion equivalents, while O_R2 binding corresponds to the displacement of 5.2 apparent ion equivalents. The near constancy of cooperative interactions is also common to all three studies. It is compelling to speculate that this set of results (pH, KCl, T) points to similar types of interaction by which sites O_R1 and O_R3 are recognized and specifically liganded.

Interpretation of the thermodynamic quantities $\Delta G°$, $\Delta H°$, and $\Delta S°$ (Table VI) in terms of the noncovalent interactions which would contribute to each parameter is difficult (Sturtevant, 1977; Ross & Subramanian, 1981). The overall process is enthalpically driven, in striking contrast with many protein–DNA reactions studied. A second notable feature is the large proton absorption (i.e., 2.1 mol/operator). If one attributed the entire enthalpic effect (i.e., −60.7 kcal/operator) to the observed proton absorption, it would require an average ionization of 30 kcal/mol H^+, which is far in excess of the value for any known group within the protein or DNA structures. A combination of hydrogen-bond formation, van der Waals interactions, and protonation is the most probable source of the large negative values of $\Delta H°$ (Ross & Subramanian, 1981). Transfer of nonpolar surface from water into the nonaqueous environment (the hydrophobic effect) would also contribute a negative enthalpic term (Baldwin, 1986; Privalov & Gill, 1988). The contribution of electrostatic interactions and counterion release (the polyelectrolyte effect) as an entropic driving force in this class of protein–DNA complexes has been well documented (Record et al., 1976, 1978; Lohman, 1985) but clearly does not dominate the energetics of this system. Ligation at each of the three sites of O_R is accompanied by the apparent release of counterions (Koblan & Ackers, 1991b). For sites O_R1, O_R2, and O_R3, $\Delta S°$ is small and negative (Table VI). One expects a positive $\Delta S°$ value for release of a cationic ligand interacting with DNA. The negative value of $\Delta S°$ at each site could arise from conformational changes within the DNA site. It is also possible that the negative contributions to $\Delta S°$ by van der Waals interactions and hydrogen-bond formation at O_R1, O_R2, and O_R3 could more than compensate for the positive $\Delta S°$ from either counterion release or hydrophobic association.

Structural Origins of the Energetic Effects. Recent structural results on the *c*I repressor N-terminal domain/O_L1 cocrystals demonstrate the complexity of protein–DNA interactions in this and similar systems (Jordan & Pabo, 1988). An extensive network of hydrogen bonds between both the edges of base pairs in the major groove and the sugar–phosphate backbone helps to stabilize the complex. In each operator half-site hydrogen bonds are made between the protein and base pairs at position 2 (A·T) and positions 4 and 6 (both G·C). These base-pair positions are strictly conserved in all but one of the half-sites which make up both O_R and the left operator, O_L. Interactions between the N-terminal domain and the sugar–phosphate backbone involve approximately 12 additional hydrogen bonds (Jordan & Pabo, 1988). The importance of hydrogen-bond formation to the overall stability in the crystal complex is entirely consistent with the experimentally determined large and negative enthalpies of the present study as noted above. Hydrophobic interactions at base positions 1, 3, and 5 of the consensus half-sites also contribute to the stability of the repressor–operator complex (consistent with thermodynamic data of this study).

Interpretation of the parallel between site O_R1 and O_R3 binding as a function of temperature, [KCl], and proton activity leads us to consider the specific DNA sequences themselves. Recent laser Raman studies of the *c*I repressor N-terminal domain interacting with sites O_L1 and O_R3 reveal that the conformation of each operator is significantly and differentially altered by repressor binding (Benevides et al., 1991). λ *cro* repressor binding induces conformational changes in the structure of a 17-bp consensus operator site (Brennan et al., 1990). Patterns obtained by driving the system with different thermodynamic potentials must correlate at some level with specific structures accessible to the system. Given the results of this study and previous studies from this laboratory (Senear & Ackers, 1990; Koblan & Ackers, 1991b), it appears that ligation of O_R1 and O_R3 may involve similar equilibria at the level of both the protein and the DNA. Conformational flexibility of the λ operators upon ligation by either *c*I or *cro* repressor may aid in discrimination of related operators (Benevides et al., 1991; Brennan et al., 1990). That sequence-dependent conformation at each of the three sites may be important for biological regulation and site-specific ligation is suggested by the results of this study.

References

Ackers, G. K., & Smith, F. R. (1987) *Annu. Rev. Biophys. Biophys. Chem. 16*, 583–609.

Ackers, G. K., Johnson, A. D., & Shea, M. A. (1982) *Proc. Natl. Acad. Sci. U.S.A. 79*, 1849–1853.

Ackers, G. K., Shea, M. A., & Smith, F. R. (1983) *J. Mol. Biol. 170*, 223–242.

Backman, K., Ptashne, M., & Gilbert, W. (1976) *Proc. Natl. Acad. Sci. U.S.A. 73*, 4174–4178.

Baldwin, R. (1986) *Proc. Natl. Acad. Sci. U.S.A. 83*, 8069–8072.

Beckett, D., Koblan, K. S., & Ackers, G. K. (1991) *Anal. Biochem. 196*, 69–75.

Benevides, J. M., Weiss, M. A., & Thomas, G. J., Jr. (1991) *Biochemistry 30*, 5955–5963.

Bevington, P. R. (1969) *Data Reduction and Error Analysis for the Physical Sciences*, McGraw-Hill, New York.

Birnboim, H., & Doly, J. (1979) *Nucleic Acids Res. 7*, 1513–1523.

Brennan, R. C., Roderick, S. L., Takeda, Y., & Mathews, B. (1990) *Proc. Natl. Acad. Sci. U.S.A. 87*, 8165-8169.
Brenowitz, M., Senear, D. F., Shea, M. A., & Ackers, G. K. (1986a) *Proc. Natl. Acad. Sci. U.S.A. 83*, 8462-8466.
Brenowitz, M., Senear, D. F., Shea, M. A., & Ackers, G. K. (1986b) *Methods Enzymol. 130*, 132-181.
Brenowitz, M., Senear, D. F., & Ackers, G. K. (1989) *Nucleic Acids Res. 17*, 3747-3755.
Chiu, R., Angel, P., & Karin, M. (1989) *Cell 59*, 979-986.
Dabrowiak, J. C., Goodisman, J., & Kissinger, K. (1990) *Biochemistry 29*, 6139-6145.
Ha, J., Spolar, R. S., & Record, M. T., Jr. (1989) *J. Mol. Biol. 209*, 801-816.
Johnson, A. (1980) Ph.D. Dissertation, Harvard University, Cambridge, MA.
Johnson, A. D., Meyer, B. J., & Ptashne, M. (1979) *Proc. Natl. Acad. Sci. U.S.A. 76*, 5061-5065.
Johnson, A., Pabo, C., & Sauer, R. T. (1980) *Methods Enzymol. 65*, 839-856.
Johnson, M. L., & Frasier, S. G. (1985) *Methods Enzymol. 117*, 301-342.
Johnson, M., Halvorson, H., & Ackers, G. K. (1976) *Biochemistry 15*, 5363-5367.
Jordan, S. R., & Pabo, C. O. (1988) *Science 242*, 893-899.
Koblan, K. S., & Ackers, G. K. (1991a) *Biochemistry 30*, 7817-7821.
Koblan, K. S., & Ackers, G. K. (1991b) *Biochemistry 30*, 7822-7827.
Koblan, K. S., Bain, D. L., Beckett, D., Shea, M. A., & Ackers, G. K. (1991) *Methods Enzymol.* (in press).
Lohman, T. M. (1985) *CRC Crit. Rev. Biochem. 19*, 191-245.
Maniatis, T., Fritsch, E. F., & Sambrook, J. (1982) *Molecular Cloning: A Laboratory Manual*, Cold Spring Harbor Laboratory, Cold Spring Harbor, NY.
Meyer, B. J., Maurer, R., & Ptashne, M. (1980) *J. Mol. Biol. 139*, 163-194.
Privalov, P. L., & Gill, S. J. (1988) *Adv. Protein Chem. 39*, 191-234.
Ptashne, M. (1967) *Nature 214*, 232-234.
Ptashne, M. (1986) *The Genetic Switch*, Cell Press, Cambridge, MA.
Record, M. T., Jr., Lohman, T. M., & deHaseth, P. L. (1976) *J. Mol. Biol. 107*, 145-158.
Record, M. T., Jr., Anderson, C. F., & Lohman, T. M. (1978) *Q. Rev. Biophys. 11*, 103-178.
Ross, P. D., & Subramanian, S. (1981) *Biochemistry 20*, 3096-3102.
Sauer, R. (1979) Ph.D. Dissertation, Harvard University, Cambridge, MA.
Schutte, J., Viallet, J., Nau, M., Segal, S., Fedorko, J., & Minna, J. (1989) *Cell 59*, 987-997.
Senear, D. F., & Ackers, G. K. (1990) *Biochemistry 29*, 6568-6577.
Senear, D. F., & Batey, R. (1991) *Biochemistry 30*, 6677-6688.
Senear, D. F., Brenowitz, M., Shea, M. A., & Ackers, G. K. (1986) *Biochemistry 25*, 7344-7354.
Shea, M. A. (1983) Ph.D. Dissertation, Johns Hopkins University, Baltimore, MD.
Shea, M. A., & Ackers, G. K. (1985) *J. Mol. Biol. 181*, 211-230.
Sturtevant, J. M. (1977) *Proc. Natl. Acad. Sci. U.S.A. 74*, 2236-2240.
Wyman, J., Jr. (1964) *Adv. Protein Chem. 19*, 224-394.

Novel DNA Superstructures Formed by Telomere-like Oligomers†

Dipankar Sen* and Walter Gilbert

Department of Cellular and Developmental Biology, Harvard University, Cambridge, Massachusetts 02138
Received July 26, 1991; Revised Manuscript Received September 26, 1991

ABSTRACT: DNA oligomers containing three or more contiguous guanines form tetrastranded parallel complexes, G4-DNA, in the presence of alkali cations. However, oligomers that have a single multi-guanine motif at their 3′ or 5′ end, with a guanine as the terminal base, also form higher order products. Thus, the oligomer T_8G_3T forms a unique G4-DNA product at neutral pH in the presence of Na^+, K^+, or Rb^+; however, its isomeric counterpart T_9G_3 in K^+ or Rb^+ generates an additional ladder of products of substantially lower gel mobility. We show that these larger complexes contain, respectively, 8, 12, or 16 distinct strands of oligomer. The octamer structure formed by T_9G_3 assembles in moderate salt at room temperature and melts around 60 °C in 100 mM KCl. Methylation protection experiments suggest a nested head-to-tail superstructure containing two tetraplexes bonded front-to-back via G quartets formed by out-of-register guanines. Naturally occurring chromosomal telomeres, which all have guanines at their 3′ termini, may be able to form these superstructures.

DNA oligomers containing one or more guanine motifs (i.e., stretches of contiguous guanines) form, in the presence of alkali cations, a family of higher order structures bonded by guanine–guanine base pairs and base quartets [reviewed recently by Guschlbauer et al. (1990), Sundquist (1991), and Sen and Gilbert (1991)]. The association of four independent strands results in the formation of G4-DNA, a complex in which the four strands run parallel, as determined by methylation protection (Sen & Gilbert, 1988; Kim et al., 1991). A notable difference appears in the conditions necessary for the formation

† This work was supported by NIH Grant 5 R01 GM41895.

0006-2960/92/0431-65$03.00/0